ANTIMICROBIAL AGENTS AND CHEMOTHERAPY, May 2004, p. 1823–1836 Vol. 48, No. 5
0066-4804/04/$08.00+0 DOI: 10.1128/AAC.48.5.1823–1836.2004

Novel Non-*mecA*-Containing Staphylococcal Chromosomal Cassette Composite Island Containing *pbp4* and *tagF* Genes in a Commensal Staphylococcal Species: a Possible Reservoir for Antibiotic Resistance Islands in *Staphylococcus aureus*

Kanokporn Mongkolrattanothai,[1]† Susan Boyle,[1]† Trudy V. Murphy,[2]‡ and Robert S. Daum[1]*

Section of Pediatric Infectious Diseases, Department of Pediatrics, University of Chicago, Chicago, Illinois,[1] and Department of Pediatrics, University of Texas Southwestern Medical Center, Dallas, Texas[2]

Received 8 September 2003/Returned for modification 30 October 2003/Accepted 21 January 2004

Among methicillin-resistant *Staphylococcus aureus* isolates, a staphylococcal chromosomal cassette containing the *mecA* gene (SCC*mec*) is integrated into the chromosome at a unique site. SCC*mec* also contains unique *ccrAB* recombinase genes mediating its integration and excision from the genome and is flanked by characteristic left and right direct- and inverted-repeat sequences. A few non-*mecA*-containing SCC elements that have the other molecular features described above have recently been described. The origin of these cassettes is not clear. We have identified two new members of the SCC family integrated within *orfX* in *Staphylococcus epidermidis* strain ATCC 12228, neither of which carries *mecA*. One is a 57-kb element flanked by a unique 28-bp SCC direct repeat. It was called the SCC composite island (SCC-CI) because it carries a 19-kb SCC element (SCC*pbp4*) nested within it. SCC*pbp4* contains *pbp4* and *tagF* genes, as well as one pair of *ccrAB* genes (allotype 2) flanked by classical SCC-specific terminal repeats. External to SCC*pbp4*, SCC-CI contains a second pair of *ccrAB* genes (allotype 4), three IS*431* elements, and genes mediating resistance to heavy metals. Genes mediating restriction-modification that may facilitate horizontal transfer are also present within SCC-CI, both within and outside SCC*pbp4*. Several novel arrangements of the SCC direct and inverted repeats were identified. Several long stretches of homology with other SCCs were found within and outside SCC*pbp4*. In view of the fact that SCC-CI was found in a commensal species, it may represent a reservoir for sequences involved in genetic shuffling between staphylococci and may contribute to the diversity found in SCC elements.

Staphylococcus aureus is an important human pathogen that causes a variety of hospital- and community-acquired infectious syndromes. Comparative analysis of three *S. aureus* genomes (3, 14) has revealed that, within a relatively constant genetic background, plasticity in the species is conferred by horizontal transfer of large genetic elements of unknown origin that insert into the genome (11). Stabilization of such elements in the genome presumably occurs when the genes that encode the transfer or excision functions, or the *cis*-acting sites on which these recombinases act, are deleted or mutated.

Resistance to methicillin in *S. aureus* is an important clinical problem because few therapeutic options exist. The methicillin resistance phenotype results from *mecA*-directed production of the transpeptidase penicillin-binding protein 2′ or 2a (PBP 2′ or PBP 2a), which has decreased affinity for β-lactam antibiotics. A site-specific integrative genetic element called staphylococcal chromosomal cassette *mec* (SCC*mec*) carries the *mecA* gene complex, which consists of the *mecA* gene itself, its regulating genes, when present, and the insertion sequence IS*431mec* (10). It also contains unique cassette chromosome recombinase genes (*ccr*) that encode products responsible for the integration and excision of the SCC*mec* element (10).

In all methicillin-resistant *S. aureus* (MRSA) isolates, SCC*mec* elements are integrated into the *S. aureus* genome at a unique site (*attBscc*) located in frame at the 3′ end of an open reading frame (ORF) of unknown function called *orfX* (10, 16). When SCC*mec* integrates, it is flanked on either end with characteristic direct- and inverted-repeat sequences (DR_{SCC} and IR_{SCC}, respectively). It is not clear how these elements are horizontally transferred, since there are no known genes encoding bacteriophage structural proteins or proteins involved in the horizontal transfer of the elements identified to date (10, 16).

SCC*mec* elements have been classified into types I to IV according to the class of *mecA* gene complex and the type of *ccr* gene complex present (11). Three relatively large SCC*mec* elements, types I, II, and III, were initially described for MRSA isolates, which were mostly obtained from patients frequenting health care environments (10). A smaller SCC*mec* element, type IV, was first identified in community-acquired MRSA (CA-MRSA) isolates from Chicago (4, 16) and was subsequently found in MRSA isolates from other geographic locales (3, 6, 18) and in *Staphylococcus epidermidis* (22).

Two other SCC elements that contain the essential features of SCC*mec* but lack the *mecA* gene have been recognized recently. SCC*cap1*, which carries the gene cluster encoding the

* Corresponding author. Mailing address: University of Chicago, Department of Pediatrics, 5841 S. Maryland Ave., MC 6054, Chicago, IL 60637. Phone: (773) 702-6176. Fax: (773) 702-1196. E-mail: rdaum@peds.bsd.uchicago.edu.

† K.M. and S.B. contributed equally to this work.

‡ Present address: National Immunization Program, Centers for Disease Control and Prevention, Atlanta, Georgia.

type 1 capsular polysaccharide, was identified in *S. aureus* strain M, a methicillin-susceptible strain (15). SCC_{12263} was recently identified in *Staphylococcus hominis* ATCC 27844. Because it carries a functional pair of *ccr* genes and other sequences with variable homology to those found in SCC*mec* elements (13), it has been proposed that SCC_{12263} may be ancestral to SCC*mec* elements.

The type IV SCC*mec* element has been of considerable interest because of its epidemiologic link to CA-MRSA and because its relatively small size makes it potentially amenable to interbacterial transfer, for example, on a bacteriophage. Molecular subdefinition of SCC*mec* type IV elements has been determined by DNA sequencing (4, 16). The DNA sequences of SCC*mec* type IV elements from two Chicago CA-MRSA isolates were highly similar to each other in all regions except the left extremity (L-C) region (16), whose sequence differences resulted in the designation of SCC*mec* IV subtypes IVa and IVb. Recently, a third subtype, IVc, also with L-C region polymorphism relative to other SCC*mec* type IV elements, was reported among MRSA isolates from France (9) and Japan (11).

It has been proposed that the L-C region contains unrelated genes and pseudogenes (9) and a number of unnecessary ORFs (16). Thus, this region has been termed a "junkyard" (9), a term suggesting functional insignificance.

We have hypothesized that the L-C region is useful for understanding the molecular epidemiology of SCC elements. While characterizing the L-C region in SCC*mec* elements in CA-MRSA isolates in our collection, we identified a ca. 9-kb sequence in one of these isolates that was found in its entirety in the sequenced genome of *S. epidermidis* ATCC 12228 and in the recently described SCC*mec* IVc element. Upon analysis of the *S. epidermidis* genome sequence flanking this ca. 9-kb homologous region, the sequence was found to be part of a unique 57-kb SCC composite island that lacked *mecA* but carried two pairs of complete *ccr* recombinase genes of different types, each contained within a region of DNA flanked by SCC-specific terminal repeat sequences. We have called this element the SCC composite island because we also found that it contained a second, smaller SCC element, SCC*pbp4*, that carried a homolog of the gene encoding PBP 4 (*pbp4*), a gene encoding a teichoic acid biosynthesis protein (*tagF*), and three stretches of DNA (>2 to 10 kb) that are highly homologous to those found in *S. aureus* SCC*mec* elements. Thus, these two new members of the SCC family found in *S. epidermidis* could be ancestral to SCC*mec* elements found in *S. aureus* by acting as a reservoir for donation of sequences to SCC elements in *S. aureus* by homologous recombination.

MATERIALS AND METHODS

Bacterial strains. The characteristics of the strains used in this study are given in Table 1. CA-MRSA isolates CA05 and 8/6-3P, recovered from children in Chicago (16), served as the prototypes of SCC*mec* types IVa and IVb, respectively. CA-MRSA isolate 2314 was isolated in 1996 from a day care center attendee in Dallas (1).

Typing of the SCC*mec* element. The *mecA* gene complex class, A or B, is assigned on the basis of the presence or absence of ψIS*1272*, *mecI*, and two functional regions of *mecR1* (17). Sequence variability in the *ccrA* and *ccrB* genes determines the assignment to *ccr* gene complex types 1 to 4 (10, 20). Typing of *mec* and *ccr* complexes is performed by PCR amplification of the relevant regions with primers described previously (10). An SCC*mec* element was classified as type IV if the type 2 *ccr* gene complex and the class B *mecA* gene complex were both detected by PCR, as described previously (4, 16). The SCC*mec* type IVa and IVb elements contain four contiguous and overlapping structural regions (from left to right, L-C, C-M, M-I, and I-R) that were screened for by PCR with region-specific primers as reported previously.

TABLE 1. Molecular characteristics of CA-MRSA isolates

Strain	Source	L-C region PCR product size (kb)		SCC*mec* subtype[a]
		cLs1–α5	cL2′–α5	
CA05	Chicago	9.9	No product	IVa
8/6-3P	Chicago	No product	9.1	IVb
2314	Dallas	3	9.6	IV

[a] Classification by SCC*mec* IV subtype (a or b). The classification scheme used by Oliveira and de Lencastre, which uses the term SCC*mec* type IVA to refer to the presence of pUB110 in the I- R region of the SCC*mec* element (19), did not apply here.

Screening for subtypes IVa and IVb was conducted with primer pairs cLs1–α5 and cL2′–α5, which amplify the L-C regions from subtypes IVa and IVb, respectively (4, 16). The L-C region spans the left extremity of the SCC*mec* element from $IRSCC_{mec}$-L to the *ccr* gene complex. We have further refined our SCC*mec* subtyping protocol by using restriction fragment length polymorphism (RFLP) to digest amplicons with the restriction endonuclease EcoRV as described elsewhere (16a). Digested fragments were separated in 0.8% agarose gels at 100 V, visualized by staining with ethidium bromide, and photographed under illumination from a UV light source. RFLP patterns were assigned by visual inspection of samples run on the same gel.

DNA sequencing. Agarose gel-purified PCR products were sequenced by using a primer-walking strategy. (Primer sequences are available upon request.) Sequencing reactions were performed by using fluorescent dideoxy chain termination chemistry and an ABI Prism sequence detection system (Applied Biosystems, Foster City, Calif.) at the University of Chicago DNA Sequencing Facility. Homology searches were performed against all sequences in the GenBank database by using the BLAST search engine, available through the National Center for Biotechnology Information (NCBI) website (http://www.ncbi.nlm.nih.gov) (2). DNA sequence alignments were performed by using ClustalW alignment software (version 1.81; Silicon Graphics) (CMBI ClustalW server) (21). ORFs in the L-C region of isolate 2314 were identified by using ORF Finder, available on the NCBI website, or by comparison to annotated gene sequences in the *S. epidermidis* ATCC 12228 (GenBank accession no. AE016744) database.

DNA sequences of the other SCC*mec* types (I to III) were obtained from GenBank. NCTC 10442 (GenBank accession no. AB033763), N315 (D86934), and 85/2082 (AB037671) sequences were used as the prototypes of SCC*mec* types I, II, and III, respectively (10). SCC*mec* type IVa was from CA-MRSA isolates CA05 (GenBank accession no. AB063172) (16) and MW2 (3); SCC*mec* type IVc was from the health care-associated MRSA (HA-MRSA) isolate MR108 (GenBank accession no. AB096217). Sequences from coagulase-negative staphylococci were from *S. epidermidis* ATCC 12228 (GenBank accession no. AE016744) (23) and *S. hominis* ATCC 27844 (AB063171).

Nucleotide sequence accession numbers. To annotate the SCC composite island and SCC*pbp4* elements that we identified in the *S. epidermidis* ATCC 12228 sequence (GenBank accession no. AE016744), a third-party annotation (TPA BK001539) was added to GenBank. The sequence of the type IV SCC*mec* element of the Dallas CA-MRSA isolate 2314 was assigned GenBank accession no. AY271717.

RESULTS

SCC*mec* typing and subtyping of CA-MRSA isolate 2314 by PCR and EcoRV RFLP. CA-MRSA isolate 2314, from a Dallas day care center attendee (1), contained an SCC*mec* type IV element with the characteristic combination of type 2 *ccr* and class B *mecA* gene complexes (ψIS*1272*-Δ*mecR1-mecA*-IS*431mec*).

PCR amplification of the L-C region of the SCC*mec* type IV element from isolate 2314 with the type IVa-specific primer pair cLs1–α5 produced a 3-kb product, which was not the

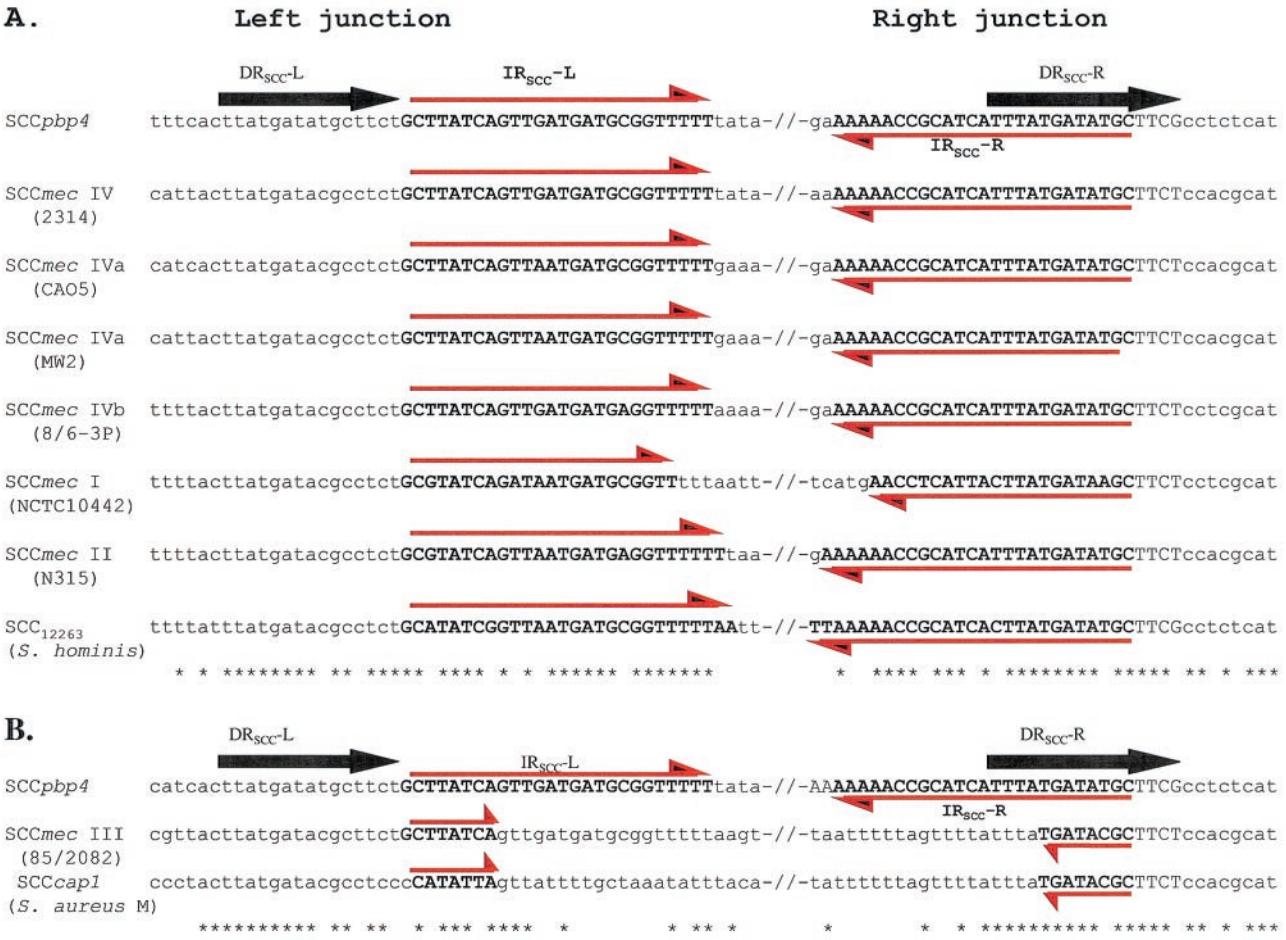

FIG. 1. Alignment of DNA sequences of DR_{SCC} and IR_{SCC} junctions from SCC and SCC*mec* elements. Shown are SCC*pbp4* alignments with SCC*mec* types I, II, and IV and SCC_{12263} (A) and with SCC*mec* type III and SCC*cap1* (B). Strains represented are isolate 2314 (SCC*mec* IV), ATCC 12228 (SCC*pbp4*), CA05 and MW2 (SCC*mec* IVa), 8/6-3P (SCC*mec* IVb), NCTC 10442 (SCC*mec* I), N315 (SCC*mec* II), 85/2082 (SCC*mec* III), ATCC 27844 (SCC_{12263}), and *S. aureus* M (SCC*cap1*). DR_{SCC} and IR_{SCC} in the left junction were designated DR_{SCC}-L and IR_{SCC}-L, respectively; DR_{SCC} and IR_{SCC} in the right junction were designated DR_{SCC}-R and IR_{SCC}-R, respectively. Capital letters, nucleotides in SCC or SCC*mec* elements; lowercase letters, nucleotides in chromosomal regions. Black arrows, direct-repeat sequences; red arrows, inverted-repeat sequences. Asterisks indicate identical nucleotides in the comparison sequences; pairs of slashes indicate intervening omitted sequences.

expected size for type IVa (Table 1). By use of the primer pair cL2′–α5, a product similar in mobility to the expected 9.1-kb fragment obtained from the IVb prototype isolate 8/6-3P was obtained. However, the EcoRV restriction fragment pattern of the amplicon from isolate 2314 differed from that of type IVb (data not shown). Thus, this isolate could not be assigned to SCC*mec* type IVa or IVb.

We sequenced the ca. 9-kb PCR product (GenBank accession no. AY271717) to further characterize the L-C region of this SCC*mec* element. The amplified fragment had 9,612 bp and contained a 15-bp SCC-specific direct-repeat sequence (DR_{SCC}-left [DR_{SCC}-L]) (nucleotides [nt] 2691 through 2705; accession no. AY271717) juxtaposed to the left extremity, a feature that is characteristic of SCC elements. Adjacent to DR_{SCC}-L was the 26-bp inverted-repeat sequence (IR_{SCC}-L; nt 2706 through 2731), also characteristic of the left termini of SCC*mec* elements (Fig. 1).

Further analysis of the 9.6-kb L-C region sequence from strain 2314 revealed that it contained a ca. 6.9-kb sequence (from accession no. AY271717, nt 2678 through 9612) that was 99% identical to a ca. 6.9-kb stretch of DNA (GenBank accession no. AB096217, nt 6487 through 13421) in the left extremity region of the recently described SCC*mec* type IVc element of HA-MRSA strain MR108 (18). Also, the same region of DNA from strain 2314 (accession no. AY271717, nt 2689 through 9612) was 99% identical to a ca. 6.9-kb stretch of DNA in the recently reported genome sequence of methicillin-susceptible *S. epidermidis* isolate ATCC 12228 (complement of nt 51523 through 44600, GenBank accession no. AE016744) that was not annotated as lying within an SCC element.

We found that that the L-C region of the SCC*mec* element of isolate 2314 contained five tandem ORFs, each encoding >50 predicted amino acids, designated ORFs 1 through 5 in succession, beginning from the left extremity (Fig. 2). The tandem architecture of the five ORFs was conserved in the L-C region of the type IVc SCC*mec* of HA-MRSA strain MR108 with 100% sequence identity. Downstream of ORF 5, there was one complete copy each of the *ccrA* and *ccrB* genes; these

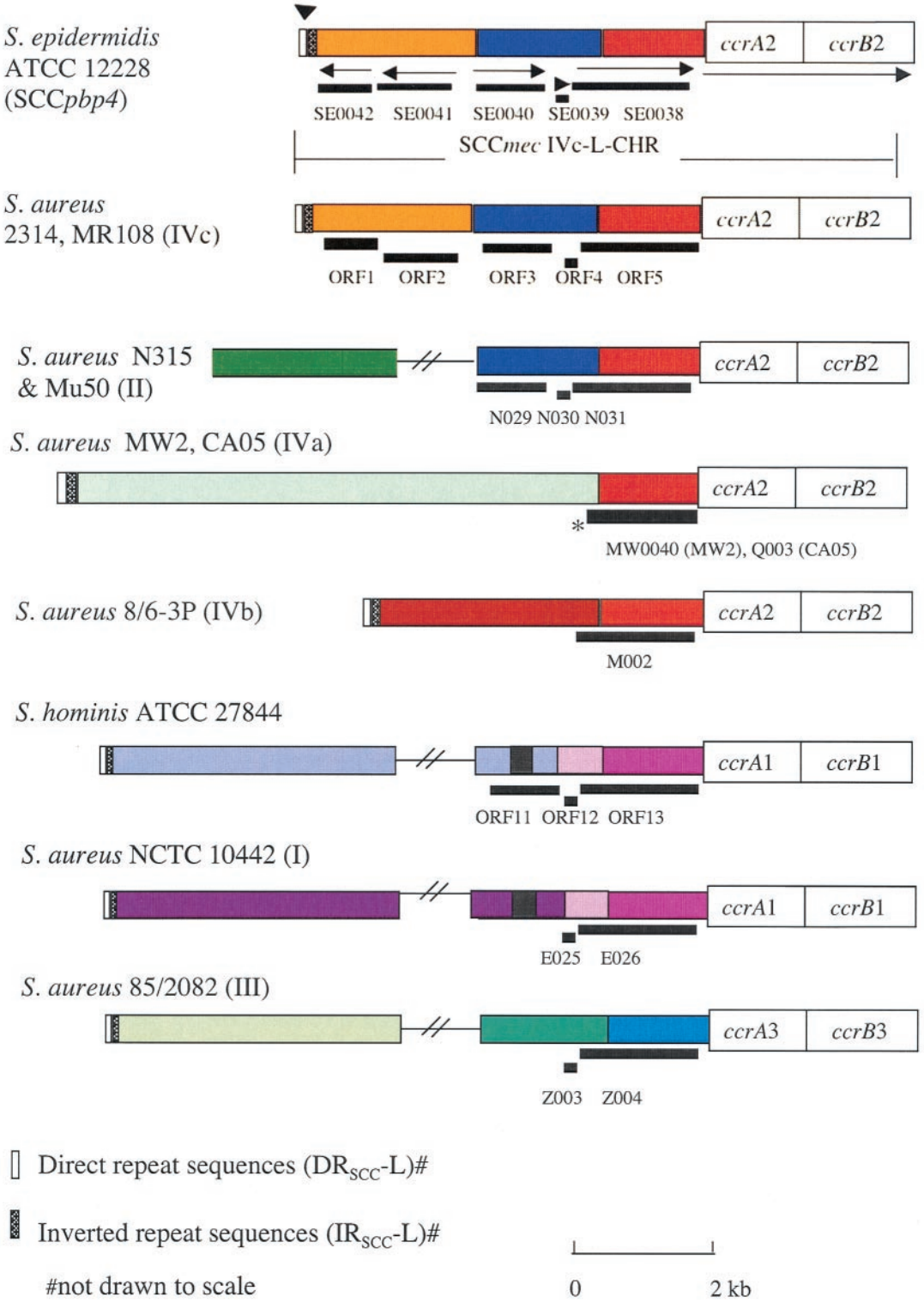

FIG. 2. Map depicting the regions of high nucleotide sequence similarity between the left portion of SCC*pbp4* (L-C region), including both *ccr* genes, and the left extremities of SCC*mec* elements and non-*mec*-containing SCC elements, based on the nucleotide sequences deposited in the DDBJ/EMBL/GenBank database under accession no. AY271717 (Dallas CA-MRSA strain 2314, SCC*mec* type IV), AB096217 (strain MR108, SCC*mec* type IVc), AE016744 (*S. epidermidis* ATCC 12228, SCC*pbp4*), D86934 (strain N315, SCC*mec* type II), AB063172 (strain CA05, SCC*mec* type IVa), AP004822 (strain MW2, SCC*mec* type IVa), AB063173 (strain 8/6-3P, SCC*mec* type IVb), AB063171 (*S. hominis* ATCC 27844, SCC_{12263}), AB033763 (NCTC 10442, SCC*mec* type I), and AB037671 (*S. aureus* strain 82/2082, SCC*mec* type III). Conserved ORFs of >99 bp are indicated by solid rectangles beneath the maps of the nucleotide sequences. Arrows above the rectangles for the map of SCC*pbp4* indicate the direction of transcription. Identical colors for sequences from different elements indicate regions of >90% nucleotide sequence homology. Asterisk indicates a 28-bp sequence identity with SE0039 from SCC*pbp4*. Vertical arrowhead indicates the junction between the left SCC element and the chromosome.

were determined by ClustalW sequence alignments (data not shown) to be of allotype 2. The chromosomal sequence flanking the left extremity of the SCC*mec* element of isolate 2314 (nt 1396 through 2690) was identical to the region in methicillin-susceptible *S. aureus* isolate 8325 immediately downstream of *orfX* (GenBank accession no. AB014440), data consistent with a perfect insertion into *orfX.* This was in contrast to the type IVc SCC*mec* element in HA-MRSA strain MR108, which was adjacent to a ca. 6.5-kb element termed IE25923, present to the left of the type IVc SCC*mec* (11).

Description of SCC*pbp4*, a novel element in *S. epidermidis* ATCC 12228. The ca. 9-kb sequence from the SCC*mec* element of *S. aureus* isolate 2314, from the left extremity to the 3′ end of the *ccrB* gene (nt 2706 to 11771, GenBank accession no. AY271717) was compared with *S. epidermidis* ATCC 12228 sequences deposited in GenBank (nt 51506 to 42441, GenBank accession no. AE016744) (24), revealing 98 to 99% nucleotide sequence similarity. In *S. epidermidis*, this region contained five ORFs, designated SE0042, SE0041, SE0040, SE0039, and SE0038, from left to right, upstream of a pair of type 2 *ccrA* and *ccrB* genes (Fig. 2). ORFs SE0042 and SE0041 corresponded to ORFs 1 and 2 of strain 2314 (Fig. 2) and were annotated in accession no. AE016744 as encoding possible phage resistance proteins, similar to the abortive phage resistance protein of *Lactococcus* species and the *Streptococcus thermophilus* Abi-alpha protein. These likely represented type I restriction system enzymes. ORFs SE0040, SE0039, and SE0038 corresponded to ORFs 3, 4, and 5 of strain 2314 and to ORFs R002, R003, and R004 of strain MR108, and they encoded hypothetical proteins (Fig. 2).

Thus, the entire L-C region and the *ccrA2* and *ccrB2* genes of the type IV SCC*mec* of CA-MRSA strain 2314 were present in the genome of *S. epidermidis* ATCC 12228 as well as in the SCC*mec* type IVc element of the HA-MRSA strain MR108. We designated this ca. 9-kb homologous region in *S. epidermidis* "the SCC*mec* type IVc L-C homologous region" (SCC*mec* IVc-L-C HR) to underscore the shared homology between these two SCC*mec* type IV elements and the related region of *S. epidermidis* (Fig. 3).

Our analysis revealed the presence of a pair of SCC-specific repeat sequences as summarized in Table 2 and annotated in our third-party annotation, accession no. BK001539. These were not annotated in the *S. epidermidis* ATCC 12228 genome sequence, but their presence suggested that an SCC-like element existed in the *S. epidermidis* isolate. No *mecA* or type 1 capsule gene sequences could be found within the flanking SCC-specific repeat sequences.

However, an ORF that was annotated as *pbp4* (SE0035; GenBank accession no. AE016744) was found immediately to the right of the type 2 *ccrB* gene (Fig. 3). The translated protein had conserved domains from β-lactamase class A enzymes and D-Ala-D-Ala carboxypeptidases that belonged to pfam groups 00144 and 00768 (Fig. 4A), respectively, from the conserved database at the NCBI. The predicted amino acid sequence of this ORF was 34 to 37% homologous to that of PBP 4 from *S. aureus* (Fig. 4B). This *pbp4* homolog, located between the characteristic SCC*mec* left and right terminal DR_{SCC} and IR_{SCC} sequences, led to our designation of this novel element in the *S. epidermidis* ATCC 12228 sequence as SCC*pbp4*. No other *pbp4* homolog could be found in the *S. epidermidis* ATCC 12228 sequence. Interestingly, the architecture of the ORFs surrounding *pbp4* from *S. epidermidis* was unlike that surrounding *pbp4* in *S. aureus* (Fig. 4C). Downstream of *pbp4* in *S. epidermidis*, there was one gene encoding a teichoic acid synthesis function (*tagF*), whereas downstream of *pbp4* in *S. aureus*, there were other genes for teichoic acid synthesis (*tagA*, *tagH*, *tagG*, *tagB*, *tagX*, and *tagD*) (Fig. 4C). Also, the ATP binding cassette protein upstream of, and in reverse orientation to, the *pbp4* gene in *S. aureus* (5, 8) was not present upstream of *pbp4* in *S. epidermidis.*

The SCC-specific DR-L (nt 51507 to 51521 in accession no. AE016744) and IR-L (nt 51506 through 51481 in accession no. AE016744) sequences adjacent to the left of the gene encoding the abortive phage resistance protein defined the left extremity of SCC*pbp4* and thus were designated $DR_{SCCpbp4}$-L and $IR_{SCCpbp4}$-L, respectively (Fig. 1 and 3; Table 2). The right extremity of SCC*pbp4* was defined by a pair of IR_{SCC} and DR_{SCC} sequences, positioned ca. 19 kb to the right of $DR_{SCCpbp4}$-L and $IR_{SCCpbp4}$-L, that were similar to the SCC*mec* IR_{SCC}-R and DR_{SCC}-R (labeled $IR_{SCCpbp4}$-R and $DR_{SCCpbp4}$-R, respectively) (Fig. 1 and 3). In SCC*pbp4*, the $IR_{SCCpbp4}$-R and $DR_{SCCpbp4}$-R sequences were in opposite orientations to each other, like the corresponding sequences at the right extremities of most *S. aureus* SCC*mec* elements, and overlapped by 11 bp (Fig. 1 and 3). Thus, SCC-specific repeat sequences defined the boundaries of SCC*pbp4*; we have annotated these in our third-party accession no. TPA BK001539 (Table 2).

To the right of *pbp4* were ORFs encoding eight hypothetical proteins, spermidine acetyltransferase, TagF, and an additional hypothetical protein abutting the $IR_{SCCpbp4}$-R sequence. Thus, SCC*pbp4* carries ORFs that encode cell wall biosynthesis proteins in addition to PBP 4.

SCC*pbp4* was found to be inserted into the same chromosomal location as SCC*cap1* in *S. aureus* and SCC_{12263} in *S. hominis*. The $DR_{SCCpbp4}$-R of SCC*pbp4* was located in an *orfX* homolog that had 91% amino acid similarity to *orfX* of *S. aureus* (Fig. 3).

Description of the SCC composite island, a second, novel element in *S. epidermidis* ATCC 12228 that encompasses SCC*pbp4*. SCC*pbp4* was found to be contained within a larger element that contained identical copies of the 28-bp sequence (5′-AAAAACCGCATCATTTATGATATGCTTC-3′) referred to as $DR_{SCC\ composite\ island}$ at both its left and right extremities (Table 2; Fig. 3). Interestingly, this 28-bp sequence was composed of the overlapping $IR_{SCCpbp4}$-R and $DR_{SCCpbp4}$-R sequences found at the right extremities of SCC*pbp4* and other SCC elements (see sequences in Fig. 1 and 3). Thus, the right extremity of the SCC composite island was also the right extremity of SCC*pbp4*. Interestingly, this 28-bp sequence has not previously been observed at the left extremity of an SCC element.

To the left of the $DR_{SCCpbp4}$-L repeat, we found an IR/DR_{SCC}-R sequence that overlapped the $DR_{SCCpbp4}$-L sequence (see Fig. 3 and Table 2). Previously, the right and left DR/IR_{SCC} regions have been found only at the right and left extremities of SCC elements, separated by at least 20 to ca. 60 kb. In this novel arrangement, the overlapping right and left SCC terminal-repeat sequences formed a 55-bp sequence (AAAAACCGCATCACTTATGATATGCTTCTGCTTAT

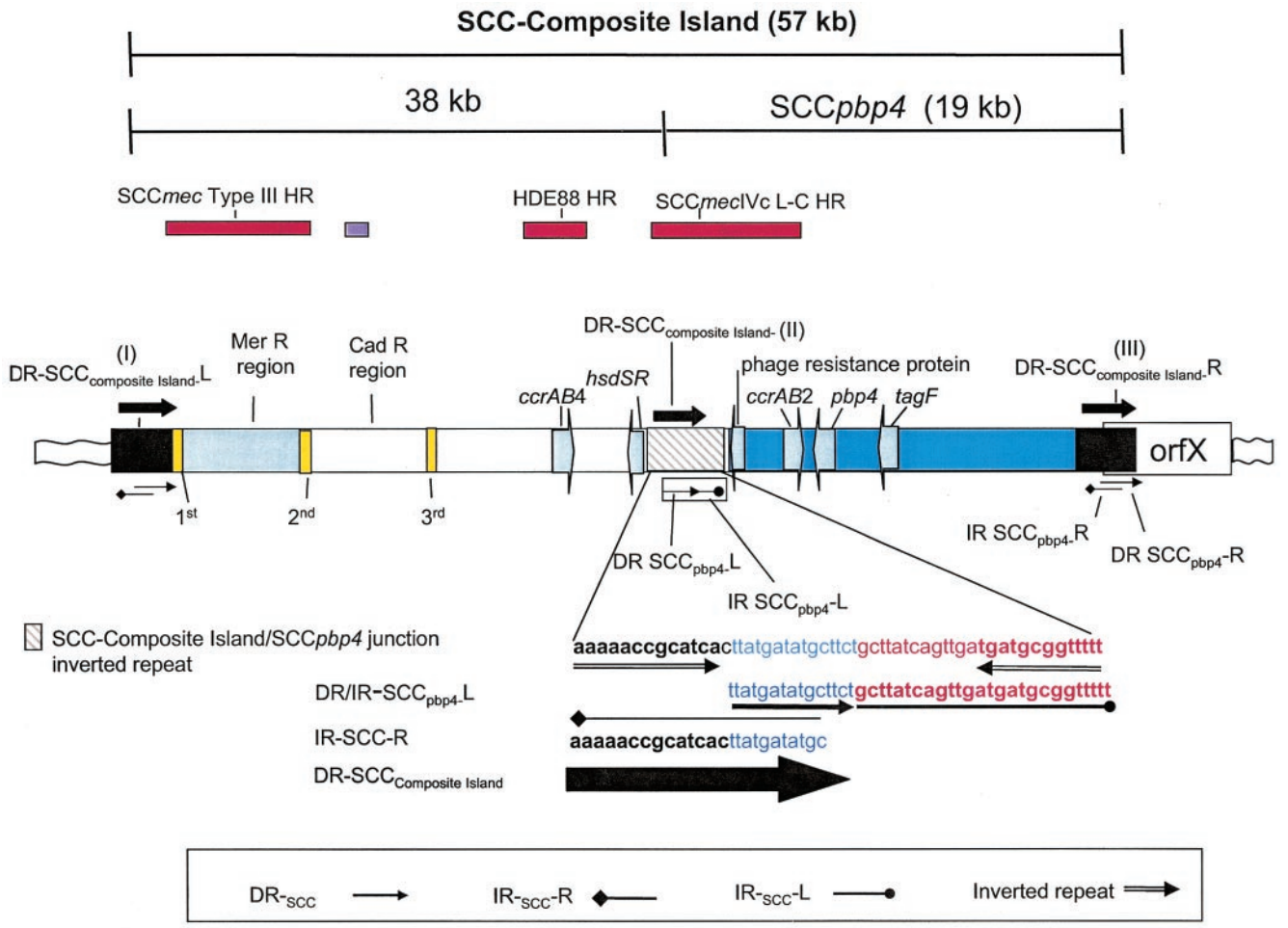

FIG. 3. Map of the 57-kb SCC composite island and the ca. 19-kb SCC*pbp4* element (dark blue background) inserted into the 3′ end of *orfX* in *S. epidermidis* ATCC 12228. The map shows the DR_{SCC}'s and IR_{SCC}'s that mark the boundaries of the elements, as well as ORFs of interest (light blue arrows showing direction of transcription). Yellow rectangles, IS*431* elements. Horizontal rectangles above the map, homologous regions (HR) of >2 kb that have 78% (lavender) to >90% (red) sequence identity to regions in the indicated SCC*mec* elements. The SCC composite island spans nt 32492 through 89965, and SCC*pbp4* spans nt 32492 to 51506, of GenBank accession no. AE016744. In order to emphasize the SCC-specific repeat regions, the map is not drawn to scale. Nucleotide positions of all ORFs that correspond to those in GenBank accession no. AE016744 are given in supplemental Table 2 (http://www.ucch.org/daum-boyle_lab-composite_island_figures/table2.htm). Nucleotide positions of the SCC direct repeats and the newly annotated features (TPA BK001539) are detailed in Table 2. MerR is the ca. 10-kb region encoding genes for mercury resistance, flanked by two copies of IS*431* (see Fig. 5). CadR is a region containing genes conferring resistance to cadmium (see Fig. 5). HDE288 HR is a 5.3-kb region with 92% nucleotide identity to a region containing type 4 *ccrA* and *ccrB* genes in the SCC*mec* element in strain HDE288 (see Fig. 6). SCC*mec* type IVc L-C HR is about 9 kb long, with 99 to 100% identity to the L-C region in type IVc SCC*mec*. The nucleotide sequence and structure of one of the three 28-bp $DR\text{-}SCC_{composite\ island}$'s are shown below the map, and the overlapping repeat sequences $DR\text{-}SCC_{pbp4}$-R (right-pointing arrow) and $IR\text{-}SCC_{pbp4}$-R (line with a diamond on the left), and $IR\text{-}SCC_{pbp4}$-L (line with a Ball on the right) contained within it, are indicated. Also shown below the map are the sequence and structure of the novel SCC repeat sequence composed of overlapping DR/IR-R and IR/DR-L SCC sequences (SCC composite island–SCC*pbp4* junction inverted repeat) that forms the 13-bp perfect inverted complementary repeat separated by 29 nt.

CAGTTGATGATGCGGTTTTT) that contained a terminal 13-bp perfect complementary inverted repeat separated by 29 nt (AAAAACCGCATCA-N29-TGATGATGCGGTTTTT). Since this repeat sequence was found at the left junction of the SCC*pbp4* element within the SCC composite island, it has been designated the SCC composite island–SCC*pbp4* junction inverted repeat. This inverted repeat was also present in the noncoding region downstream of a gene encoding abortive phage resistance protein and upstream of the *hsdSR* operon, encoding type I restriction proteins (Fig. 3), suggesting that it could contain a transcriptional terminator for the former.

Further defining the SCC composite island was a second pair of *ccrA* and *ccrB* recombinase genes to the left of SCC*pbp4* (Fig. 3) that were closely related to the newly identified type 4 *ccrA* and *ccrB* allotypes (see Fig. 6) found in the SCC*mec* element of MRSA strain HDE288 (20), the so-called pediatric clone. A truncated copy of another *ccrA* gene, which was too short to assign to an allotype, was also present. In addition, there were 3 copies of a transposase for an insertion sequence-like element that we have annotated as IS*431* (TPA BK001539) and ORFs (see supplemental Table 2 at http://www.ucch.org/daum-boyle_lab-composite_island_figures/table2.htm) that en-

TABLE 2. Locations of features in SCC composite island documented in TPA BK001539

Feature	nt location in:		Characteristic or DNA sequence (5′–3′) complement
	BK 001539	AE 016744	
SCC elements			
SCC composite island	1–57474	32492–89965	
SCC*pbp4* element	1–19015	32492–51506	
L-C homologous region	9950–19015	42441–51506	Similar to L-C regions of SCC*mec* type IV
ccrAB4 homologous region	24565–29904	57056–62395	Similar to nt 6986–12345 of strain HDE288 (accession no. AF411935)
CadR homologous region	38639–41107	73585–76053	78% similarity to CadR region in SCC*mec* type III
MerR homologous region	57475–66754	80621–89900	92% similarity to MerR region in SCC*mec* type III
SCC repeat sequences			
$DR_{SCC\ composite\ island}$-R (III)	1–29	32492–32520	AAAAACCGCATCATTTATGATATGCTTCG
$DR_{SCCpbp4}$-R	1–15	32492–32506	TTATGATATGCTTCG
$DR_{SCC\ composite\ island}$ (II)	19016–19044	51507–51535	AAAAACCGCATCACTTATGATATGCTTCT
$IR_{SCCpbp4}$-L	18990–19015	51481–51506	GCTTATCAGTTGATGATGCGGTTTTT
$DR_{SCCpbp4}$-L	19016–19030	51507–51521	TTATGATATGCTTCT
SCC composite island–SCC*pbp4* junction inverted repeat	18990–19044	51481–51535	AAAAACCGCATCACTTATGATATGCTTCTGCTTATCAGTTGATGATGCGGTTTTT
DR_{SCC}-L (1 bp mm)	57448–57460	89939–89951	TTATGATATGCTTCA
IR_{SCC}-L	57450–57474	89941–89965	AAAAACCGCATCATTTATGATATGC
$DR_{SCC\ composite\ island}$-L (I)	57446–57474	89937–89965	AAAAACCGCATCATTTATGATATGCTTCA
IS*431* elements			
IS*431*-3	37850–38638	70341–71129	
IS*431*-2	48131–48919	80622–81410	
IS*431*-1	56620–57409	89111–89900	

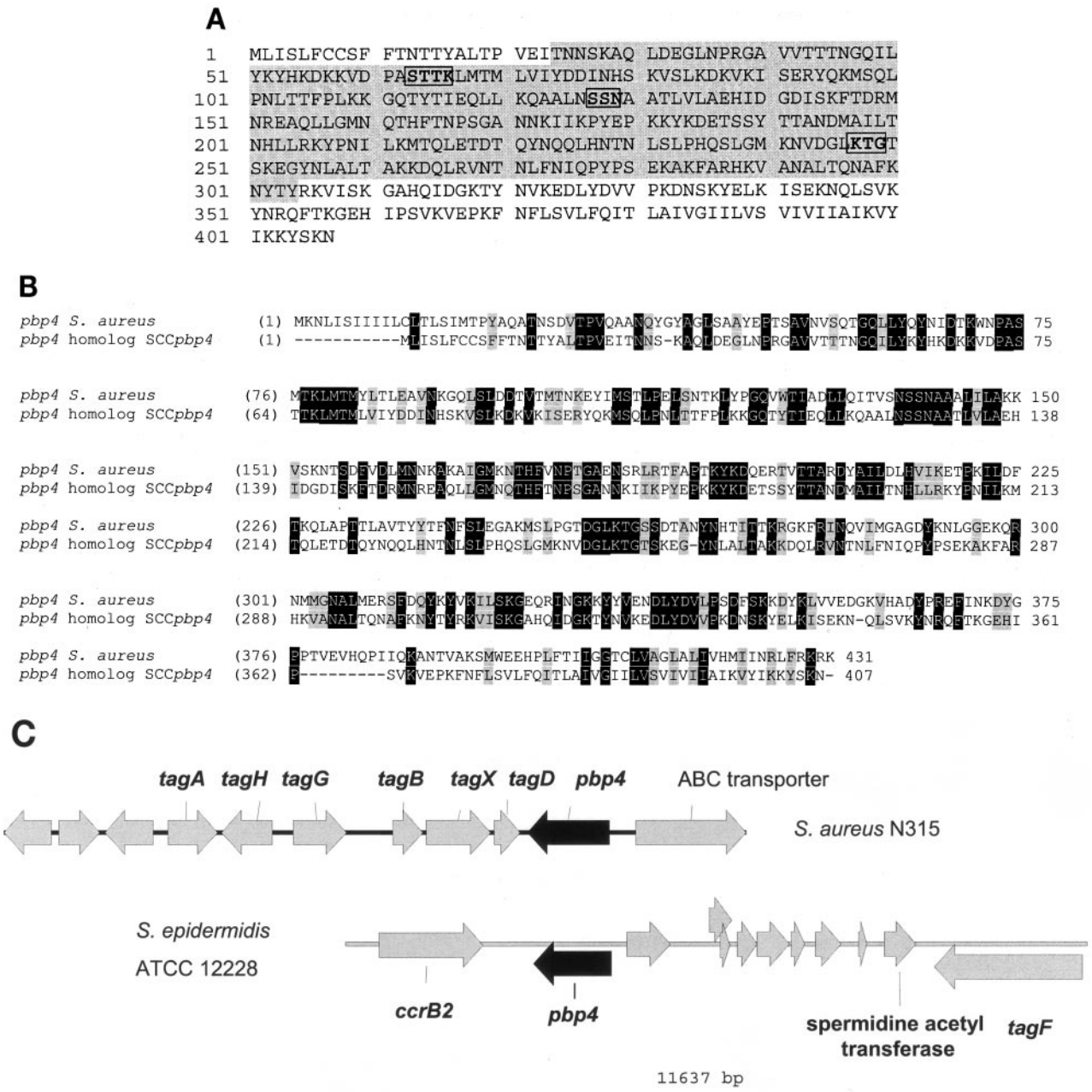

FIG. 4. Analysis of the *pbp4* homolog of SCC*pbp4*. (A) Theoretical translation of the *pbp4* homolog of *S. epidermidis* ATCC 12228, highlighting functional domain architecture. Shading indicates the peptidase S_1 domain, starting at aa 24 and ending at aa 304. The penicillin-binding domains, SXXK, SSN, and KTG, are boxed. (B) ClustalW alignment of the *pbp4* genes of *S. aureus* (GenBank accession no. SAPBP4GEN) and SCC*pbp4* of *S. epidermidis* ATCC 12228. White letters on solid background, identical residues; letters on shaded background, conservative replacements. Overall there were 46.2% similarity and 32.7% identity between the two sequences. Pairwise alignments were performed with the Vector NTI suite, version 8 (Informax, Inc.), by using the blosum62mt2 matrix. (C) Architecture of ORFs in the DNA sequences surrounding and including the *pbp4* genes (solid arrows) in *S. aureus* strain N315 (nt 91873 to 93737; accession no. AP003131) and the SCC*pbp4* element of *S. epidermidis* ATCC 12228. Arrows indicate ORFs and their direction of transcription.

code cadmium resistance, mercury and heavy-metal transport proteins, the type I restriction system proteins HsdR and HsdS, truncated transposases, another copy of spermidine acetyltransferase, and 20 hypothetical proteins. As shown in Fig. 3, many of these features in the SCC composite island are present in other members of the SCC family.

Shown in supplemental Table 2 (at the URL given above) are the locations of all ORFs present in the SCC composite island and the degrees of similarity of their translated proteins to the products of similar ORFs found in other SCC elements. Of particular interest was a ca. 9.3-kb region at the left extremity of the SCC composite island (nt 89900 to 80621, GenBank accession no. AE016744) encoding mercury resistance proteins. This region contained six ORFs encoding hypothetical

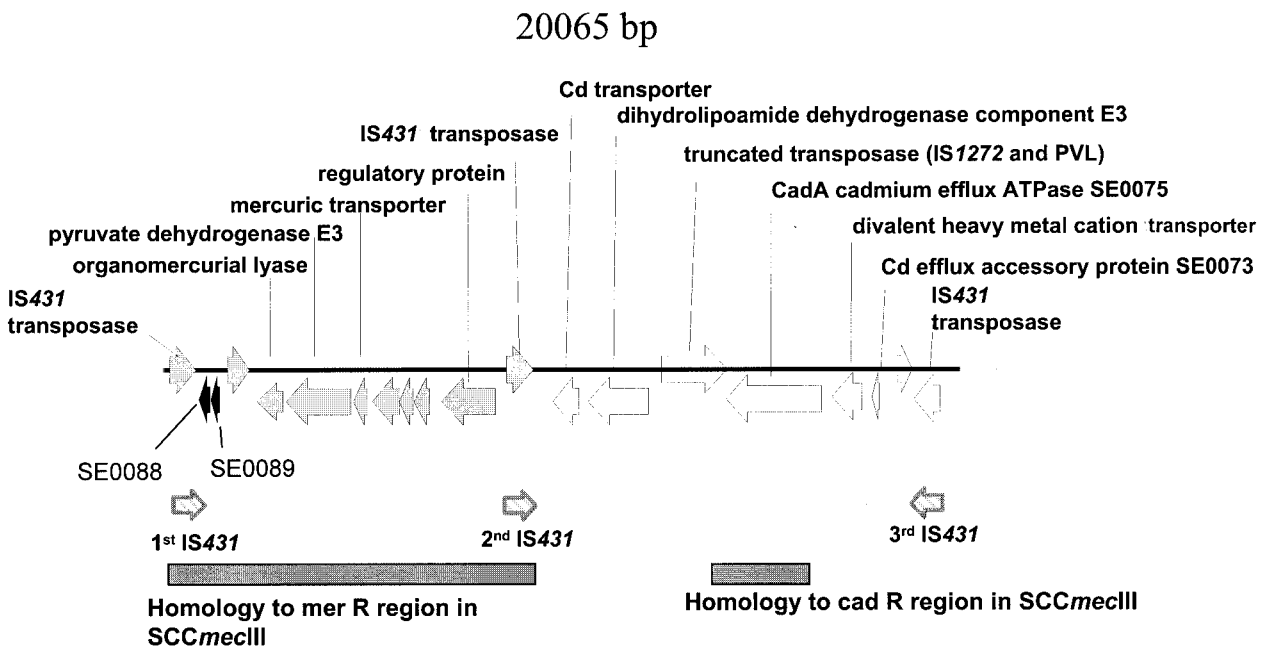

FIG. 5. Map showing the region of the SCC composite island containing three IS*431* elements (hatched arrows) and the intervening genes encoding proteins conferring heavy metal resistance (also shown, in less detail, in Fig. 3). Directions of arrows indicate the orientations of the ORFs. Shaded arrows, ORFs within a ca. 9-kb region with 99% similarity to the Mer resistance region (mer R) in SCC*mec* type III of strain 85/2082 (nt 36002 to 44579, GenBank accession no. AB037671); the region is indicated below the map. Open arrows, ORFs encoding cadmium resistance proteins. The ca. 2.3-kb region with 78% nucleotide identity with the cadmium resistance region (cad R) in SCC*mec* type III is indicated below the map. The two unique ORFs (SE0089 and SE0088, encoding hypothetical proteins with no homolog in the mer R region of SCCmec type III) are indicated by solid black arrows.

proteins and was flanked by the first and second copies of IS*431*. The region was 91.6% identical to the *mer* operon region in SCC*mec* type III of strain 85/2082 (nt 36066 to 44580, GenBank accession no. AB037671) (Fig. 5). The main difference found between the Mer regions of SCC*mec* type III and the SCC composite island was the presence of two additional ORFs (SE0089 and SE0088), located to the right of the first IS*431* element in the SCC composite island, encoding hypothetical proteins that were not present in type III SCC*mec* of strain 85/2082 (Fig. 5). Furthermore, cadmium resistance proteins (CadR region) were encoded between the second and third IS*431* elements (Fig. 3 and 5). The products of ORFs SE0075 and SE0073 (Fig. 5), encoding a putative cadmium resistance transporter and a cadmium efflux protein, respectively, were 90% similar to that encoded by ORF Z020 and 80% similar to that encoded by a portion of ORF Z019 from SCC*mec* type III (Fig. 3 and 5). Also, the CadR region contains a 2,469-bp stretch (nt 73585 through 76053, GenBank accession no. AE016744) with 75% nucleotide identity to the CadR region encompassing ORFs Z020 and Z019 in the SCC*mec* III element of strain 85/2082 (Fig. 3 and 5).

In a pairwise alignment, we also identified a 5.3-kb stretch of 92% sequence identity (Fig. 6A) between nt 57056 to 62395 (complement, GenBank accession no. AE016744) of the SCC composite island and nt 6986 to 12345 (GenBank accession no. AF411935) of SCC*mec* of strain HDE288 (the so-called pediatric MRSA clone). This region contained the type 4 *ccrA* and *ccrB* genes and flanking nucleotide sequences mentioned above (Fig. 6).

A third important stretch of similarity between other SCC elements and the SCC composite island was the ca. 9-kb region at the left extremity of SCC*pbp4* referred to as the L-C HR, mentioned above (Fig. 3).

In summary, a large, novel composite island was found in the genome sequence of *S. epidermidis* ATCC 12228. This composite island lacks *mecA* but contains two pairs of *ccr* recombinases of different allotypes (*ccrA2*/*ccrB2* and *ccrA4*/*ccrB4*) described previously in SCC*mec* elements in *S. aureus*. Nested within the composite island was a smaller (19-kb) element, SCC*pbp4*, that had a ca. 9-kb stretch of sequence homology 98 to 99% similar to a region in the SCC*mec* element of a CA-MRSA strain that harbors an SCC*mec* type IV element and of an HA-MRSA isolate that harbors type IVc SCC*mec* (11). Furthermore, outside the SCC*pbp4* region, at the left extremity, genes that encoded resistance determinants against toxic heavy metals, identical to those found in the large *S. aureus* type III SCC*mec*, were identified.

Conservation of repeat sequences and L-C region ORFs in the SCC composite island and other members of the SCC family among staphylococci. (i) Repeat elements. The IR_{SCC}-R sequences of SCC*pbp4* of *S. epidermidis* were more closely related to those in SCC*mec* type I, II, and IV (Fig. 1A) than those in SCC*mec* type III and SCC*cap1* (Fig. 1B). In contrast, the IR_{SCC}-L of SCC*pbp4* was closely related to that of SCC*mec* type III as well as types I, II, and IV but was unrelated to the IR-L of SCC*cap1*.

The 15-bp DR_{SCC}-L in CA-MRSA strain 2314 contained two mismatches with the 15-bp $DR_{SCCpbp4}$-L contained in

SCC*pbp4* in *S. epidermidis* ATCC 12228. The 26-bp $IR_{SCCpbp4}$-L of *S. epidermidis* ATCC 12228 was 100% identical to the IR_{SCC}-L's in the SCC*mec* elements of strain 2314 and similar to other MRSA isolates (N315, CA05, MW2, 8/6-3P) (3, 10, 16).

(ii) Comparison of ORFs with those in other SCC elements. Inspection of the aligned regions from the left extremities of many SCC elements depicted in Fig. 2 and the data in supplemental Table 2 (available at the URL given above) suggests a model by which SCC*mec* elements may have evolved from the SCC*pbp4* element in the 57-kb SCC composite island of *S. epidermidis*. As noted, all five ORFs (shown as solid rectangles in Fig. 2) present in the L-C HR of the SCC composite island were conserved in the L-C region of two SCC*mec* type IV elements in strain 2314 and SCC*mec* IVc in strain MR108. ORFs SE0042 and SE0041, encoding abortive phage resistance protein and Abi-alpha protein, annotated in the sequence of *S. epidermidis* ATCC 12228, were not found in any other SCC element except SCC*pbp4*, SCC*mec* IV in strain 2314, and SCC*mec* IVc in strain MR108. It is possible that these two ORFs were either lost by deletion from a primordial element such as SCC*pbp4* or gained by homologous recombination. An ORF with a high degree of similarity to SE0040 was found in five SCC elements: the type II SCC*mec* elements of N315 and Mu50, the type IV SCC*mec* elements of strains 2314 and MR108, and the SCC element found in *S. hominis*. ORFs homologous to ORF SE0039 were found in nine SCC elements: SCC*mec* type II of strains Mu50 and N315, SCC*mec* type IV of strains 2314 and MR108, SCC*mec* IVa of strains CA05 and MW2, SCC*mec* type I of strain NCTC 10442, SCC*mec* type III of strain 85/2082, and SCC_{12263} of *S. hominis*. ORFs similar to SE0040, SE0039, and SE0038 were present together in only four of the SCC elements identified to date.

Homologs of the ORF (SE0038) closest to the *ccrA2* genes were present in all SCC elements, including SCC*mec* types I, II, III, and IV, SCC*pbp4*, and SCC_{12263}, with various degrees of conservation. ORF SE0038 of *S. epidermidis* ATCC 12228 was highly conserved (97% identity) in strains 2314 (ORF 5), MR108 (ORF R004), and N315 (ORF N031). In contrast, the nucleotide and predicted amino acid sequences of these ORFs in strain 2314 and strain MR108 differed considerably at the 5′ end of the gene (from the start codon to bp 450 to 550) and the amino terminus of the translated protein from the corresponding ORFs in the type IVa SCC elements of isolates MW2 (ORF MW0040) and CA05 (ORF Q003), and the type IVb SCC elements of isolate 8/6-3P (ORF M002). Nevertheless, the 3′ terminus of this ORF in CA-MRSA strain 2314 was 95 to 96% identical to those of CA-MRSA isolates MW2, CA05, and 8/6-3P. Thus, surprisingly, ORF 5 of CA-MRSA strain 2314 was more closely related to the corresponding ORFs of *S. epidermidis* ATCC 12228 and HA-MRSA strains with type II SCC*mec* (N315 and Mu50) than to those in CA-MRSA strains with either SCC*mec* subtype IVa (MW2 and CA05) or IVb (strain 8/6-3P) or SCC*mec* type I or III.

Interestingly, the 3′ terminus of ORF SE0038 in *S. epidermidis* ATCC 12228 is conserved among SCC elements that have the type 2 *ccr* gene complex but is less similar to the corresponding ORFs contained in SCC elements carrying the type 1 or type 3 *ccr* gene complex. The 3′ terminus of ORF 5 of CA-MRSA strain 2314 was 89% similar to the correspond-

A

```
HDE288      ATGAAACAACTCAAAAAGAAACGTATTGGATTATACGCACGTGTATCAACTGAAATGCAA 60
SCC-CI      ATGAAACAACTCAAAAAGAAACGTATTGGATTATATGCACGTGTATCGACTGAAATGCAA 60
            ************************************ ************ ************

HDE288      ACGGATGGTTACAGTATTCAAGGTCAATTAAACCAACTTACAGAGTATTGTCAATTTCAA 120
SCC-CI      ACGGATGGTTACAGTATTCAAGGTCAATTGAATCAACTTACAGAGTATTGTCAATTTCAA 120
            ******************************** ** ****************************

HDE288      GGATATGAAGTCGTTGATGAATATACCGATCGAGGTATATCGGGTAAAACAATGCAACGT 180
SCC-CI      GGCTATGAAGTCGTCAATGAATACACCGATCGTGGTATATCAGGTAAAACAATGCAACGT 180
            ** ************  ******* ******** ******** ******************

HDE288      CCAGAATTACAACGTATGTTAAAAGATGCCAACGAAGGTAAATTAGATTGTATTATGGTC 240
SCC-CI      CCAGAATTACAACGTATGTTAAAAGATGCCAACGAAGGTAAATTAGATTGTATTATGGTC 240
            ************************************************************

HDE288      TACAAAACCAATCGTTTAGCTAGAAATACCTCAGATTTGTTAAATATTGTCGAGGAATTG 300
SCC-CI      TACAAAACAAATCGTTTAGCTAGAAATACCTCAGATTTGTTAAATATTGTCGAGGAATTG 300
            ******** ****************************************************

HDE288      TATAAGATTAATGTCGAATTTTTTAGTCTCACTGAAAAAATAGAAATTGCCAGCTCCACA 360
SCC-CI      TATAAGATTAATGTCGAATTTTTTAGTCTAACTGAAAAAATAGAAATTGCCAGTTCAACA 360
            ********************************* ********************** ** ***

HDE288      GGTAAGTTGATGCTCCAAATTTTAGCCAGCTTCGCAGAATTTGAAAGAAATACGATTGTA 420
SCC-CI      GGTAAATTGATGCTCCAAATTTTAGCCAGCTTCGCAGAATTTGAACGTAATACGATTGTA 420
            ***** ****************************************** * ************

HDE288      GAGAATGTCTACAATGGCCAAAGACAACGTGCGATTGAAGGTTATTATCAAGGTAATTTG 480
SCC-CI      GAGAATGTCTACAATGGCCAAAGACAACGTGCTATTGAAGGTTATTATCAAGGTAATTTA 480
            ************************************ ************************

HDE288      CCTCTAGGCTATGATAAAGTACCTGATAGTAAAAAAGAGCTCATGATTAATCAACATGAA 540
SCC-CI      CCTCTAGGCTACGATAAAGTACCTGACAGTAAAAAAGAGCTCATGATCAATCAACATGAA 540
            ********** ************** ********************** ************

HDE288      GCGAATATTGTTAAATATATCTTTAAGTCATACGCCAAAGGTCATGGTTATCGTAAGATT 600
SCC-CI      GCGAATATTGTTAAATATATTTTTGATTCATACGCTAAAGGTCATGGTTATCGTAAGATT 600
            ********************* *** * ******** ************************

HDE288      GCGAACGCATTGAATCATAAAGGTTATGTGACTAAGAAAGGGAAACCGTTTAGTATTTCA 660
SCC-CI      GCGAACGCATTGAATCATAAAGGTTATGTGACTAAGAAAGGGAAACCTTTTAGTATTTCG 660
            ************************************************ ************


HDE288      TCCATTACTTATATCATCTCAAACCCTTTTTATATTGGAAAGATACAGTTTGCGAAGTAT 720
SCC-CI      TCCATTACCTACATCATCTCAAACCCTTTTTACATTGGAAAGATACAGTTTGCGAAGTAT 720
            ******** ** ********************** ******************************

HDE288      AGACACTGGAGCGATAAGAGACGAAAAGGACTCAATGAGGAACCCATTATTGCTGATGGT 780
SCC-CI      AGACACTGGAGCGATAAAAGACGAAAAGGACTCAATGAGGAACCGATTATCGCTGATGGT 780
            ***************** ***************************** ***** **********

HDE288      AAGCATGCACCTATTATTGATAAAGCTTTATGGGATAAAGTACAGTTTAAACGCCAAGAG 840
SCC-CI      AAACATGCGCCTATTATTGATAGAAACCTATGGGATAAAGTACAGTTTAAACGTCAAGAG 840
            ** ***** ************* *    ************************** ******

HDE288      AGTCGCAAGAAACCTCAAGTTCATGGTAAAGGGACCAATCTACTGACTGGAATTGTAAAG 900
SCC-CI      AGTCGCAAGAAACCACAAGTTCACGGCAAAGGAACAAACCTACTGACTGGGATTGTAAAA 900
            ************** ******** ** ***** ** ** ********** ********

HDE288      TGCCCAAAATGTGGTGCAGCCATGGCGGCAAGTAATACAACCAATACGTTAAAAGATGGC 960
SCC-CI      TGTCCGAAATGTGGTGCAGCAATGGAGGCAAGTAATACAACTAATACATTAAAAGATGGC 960
            ** ** ***************** **** ********** ***** ************

HDE288      ACTAAGAAAAGAATCAGATATTACTCATGTAGTAATTTTAGAAACAAAGGTTCTAAAGTA 1020
SCC-CI      ACTAAGAAAAGAATCAGATATTACTCATGTAGCAATTTTAGAAATAAAGGTTCAAAAGTT 1020
            ************************************ ********** ******** *****

HDE288      TGTTCAGCCAATAGTGTTAGAGCAGATGTATTAGAAAAATATGTTATGGATCAGATATTG 1080
SCC-CI      TGTTCTGCCAATAGCGTTAGAGCAGATGTACTAGAAAAATATGTTATGGATCAGATATTG 1080
            ***** ******** ***************** ******************************

HDE288      GAAATTATCAAAAGTAAAAAGGTATTGAAACAATTGGTTGAAAAGGTAAATAAAAAAAGT 1140
SCC-CI      GAAATTATCAAAAGCAAAAAGGTATTGAAGCAATTGGTTGAAAAGGTAAATGAAAAAAGT 1140
            ************** ************** ********************** ********

HDE288      CAAATAGACGTCTCTTCTTTGAATCATGATATTGCCTATAAACAGTCACAATGTGAAGAA 1200
SCC-CI      CAAATAGACGTCTCTTCTTTGAACCATGATATTGCCTATAAACAGTCACAATGTGAAGAA 1200
            ************************ ************************************

HDE288      ATAAAAGCCAAAATGCATACACTAACGAAAACCATCGAAGACTCACCTGACTTAGATAGC 1260
SCC-CI      ATAAAAGCAAAAATGCATACATTAACGAAAACTATTGAAGACTCACCTGACTTAGATAGC 1260
            ******** ************ ********** ** ************************

HDE288      GTATTGAAACCAACAATACTTAGCTACCAAGATGAATTGAATCAAATAAATAATCAAATA 1320
SCC-CI      GTATTAAAACCAACAATACTTAGCTACCAAGATGAATTGAATCAAATAAATAATCAAATC 1320
            ***** ******************************************************

HDE288      CATCA-CTAGAACAAGATAAACAAGCAGAAGCTCCACATTATGATGCTGATATGATTGCC 1379
SCC-CI      TATCAACTAGAACAAGATAAACAAGCAGAAGCTCCACATTATGATGCTGATATGATTGCG 1380
             **** ************************************************** *

HDE288      AACGTACTACAAGCAATATTCAAAGATATAGACAAATTAGAGAAATCTCAGTTGAAATCA 1439
SCC-CI      AATGTACTACAAGCAATATTCAAAGATATAGACAAATTAGAGAAATCTCAGTTGAAATCA 1440
            ** ************************************************** *******

HDE288      CTCTATCTGACAGTTATCGATCGTATTGATATCCGAAAACATGAACATCATAAGAAGCAA 1499
SCC-CI      CTATATCTAACAATCATCGATCGCATTGACATAAGAAAAGATGAGCATCATAAGAAGCAA 1500
            ** ***** *** * ******** ***** **  ***** **** ***************

HDE288      TTTTATGTTACGCTCAAATTGAATAACGATATTATTAAACAACTATTTGATAATCATCCA 1559
SCC-CI      TTTTATGTTACGCTCAAGTTAAATAATGATATAATCAAACAACTATTTAATAACCATCCA 1560
            ****************** ** ***** ***** ** ************ **** ******

HDE288      CTTGACGAAGTGCTCCTTAGCACTTCGTCTTTATTTTTGTCCCAAACTTTATATATAACT 1619
SCC-CI      CTCGACGAAGTGCTCCCTAGCACTTCGTCTTTATTTTTGCCACAAACTTTATATATAACT 1620
            ** ************ ************************ * ******************

HDE288      ATTGAATAAA 1629
SCC-CI      ATTGAATAA- 1629
            *********
```

B

```
Translation of ccrA4 ATCC12228     (1) MEEAIAYVRQSTLKQQSLATQKSLIMDTAKQYGWSNVAFYDDKKTGRHTKRSGYQKMVEIITSGKCKVLCCYRLN 75
Translation of ccrA4 HDE288        (1) MEEVIAYVRQSTLKQQSLATQKSLIMDTAKQYGWSNVTFYDDKRSGRNTKRSGYKKIVEIITSGKCKVLCCYRLN 75

Translation of ccrA4 ATCC12228    (76) RLHRNLKNAIQFFEICKKHHITIISVNDGYFDLSKEFDCFRLNILMSLAEMESNNISEQTKNGIREKAKQGKLIT 150
Translation of ccrA4 HDE288       (76) RLHRNLKNAIQFFEICKKHHVTIISVNDGYFDLSKEFDRFRLNILMSLAEMESNNISEQTRNGIREKAKQGKLIT 150

Translation of ccrA4 ATCC12228   (151) THAPFGYRYRKGCFVVQEEEAYTVKSVYRWYLQGLGYKKISQHLDSNPNLIPRKPYQVRNILLNPNYCGRVINKY 225
Translation of ccrA4 HDE288      (151) THAPFGYRYRQGSFVVYEEEVHTVKAVYRLYLQGLGYKKISQHLDNNSKLIPRKPYQVRNILLNPNYCGRVINKY 225

Translation of ccrA4 ATCC12228   (226) GTFNDIVPPIIDIDTFEEAQERRIHKQLNRSNSRNKLKRRIKCPYCQSTLTNLTIKKENYSLRYYVCPKNMNDAY 300
Translation of ccrA4 HDE288      (226) GTFNNIVPPIIDVDTFEEAQERRIHKQHNRSNSRNKLKRRIKCPYCQSTLTNLTIKKEHHSLRYYVCPKNMNDAY 300

Translation of ccrA4 ATCC12228   (301) RTCPFKSINAPELESEVLDTCKKYFEEQSFHKRLNNTILKVLKQQQMKHKETHLTQEQLIEKLAQNRIDVKTFKR 375
Translation of ccrA4 HDE288      (301) RTCPFKGINAPELESKVLDTCKKYFEEQSFHNRLNDTILKVLKQQQMKHRQSHLTQEQLIEKLAQNQIDIETFKR 375

Translation of ccrA4 ATCC12228   (376) LSASCKSEENYSTYSTYQIDDKLKYVIKNKITLQDIAEFIDCIKITQTKQLQGIYFKNSPLNIVEQSHLITPERN 450
Translation of ccrA4 HDE288      (376) LSISYESEERYSNYSHKQMAEAVRHVIKDKLTLETIAELLDDITTQTKQLQRIYFKNSPFNIVEQSHLITPERN 450

Translation of ccrA4 ATCC12228   (451) EVI
Translation of ccrA4 HDE288      (451) EVI


Translation of ccrB4 ATCC12228     (1) MKQLKKKRIGLYARVSTEMQTDGYSIQGQLNQLTEYCQFQGYEVVNEYTDRGISGKTMQRPELQRMLKDANEGKL 75
Translation of ccrB4 HD2E88        (1) MKQLKKKRIGLYARVSTEMQTDGYSIQGQLNQLTEYCQFQGYEVVDEYTDRGISGKTMQRPELQRMLKDANEGKL 75

Translation of ccrB4  ATCC12228    (76) DCIMVYKTNRLARNTSDLLNIVEELYKINVEFFSLTEKIEIASSTGKLMLQILASFAEFERNTIVENVYNGQRQR 150
Translation of ccrB4 HD2E88        (76) DCIMVYKTNRLARNTSDLLNIVEELYKINVEFFSLTEKIEIASSTGKLMLQILASFAEFERNTIVENVYNGQRQR 150

Translation of ccrB4  ATCC12228   (151) AIEGYYQGNLPLGYDKVPDSKKELMINQHEANIVKYIFDSYAKGHGYRKIANALNHKGYVTKKGKPFSISSITYI 225
Translation of ccrB4 HDE288       (151) AIEGYYQGNLPLGYDKVPDSKKELMINQHEANIVKYIFKSYAKGHGYRKIANALNHKGYVTKKGKPFSISSITYI 225

Translation of ccrB4  ATCC12228   (226) ISNPFYIGKIQFAKYRHWSDKRRKGLNEEPIIADGKHAPIIDRNLWDKVQFKRQESRKKPQVHGKGTNLLTGIVK 300
Translation of ccrB4 HDE288       (226) ISNPFYIGKIQFAKYRHWSDKRRKGLNEEPIIADGKHAPIIDKALWDKVQFKRQESRKKPQVHGKGTNLLTGIVK 300

Translation of ccrB4  ATCC12228   (301) CPKCGAAMEASNTTNTLKDGTKKRIRYYSCSNFRNKGSKVCSANSVRADVLEKYVMDQILEIIKSKKVLKQLVEK 375
Translation of ccrB4 HDE288       (301) CPKCGAAMAASNTTNTLKDGTKKRIRYYSCSNFRNKGSKVCSANSVRADVLEKYVMDQILEIIKSKKVLKQLVEK 375

Translation of ccrB4 ATCC12228    (376) VNEKSQIDVSSLNHDIAYKQSQCEEIKAKMHTLTKTIEDSPDLDSVLKPTILSYQDELNQINNQIYQLEQDKQAE 450
Translation of ccrB4 HDE288       (376) VNKKSQIDVSSLNHDIAYKQSQCEEIKAKMHTLTKTIEDSPDLDSVLKPTILSYQDELNQINNQIHH-------- 442

Translation of ccrB4 ATCC12228    (451) APHYDADMIANVLQAIFKDIDKLEKSQLKSLYLTIIDRIDIRKDEHHKKQFYVTLKLNNDIIKQLFNNHPLDEVL 525
Translation of ccrB4 HDE288       (443) ----------------------------------------------------------------------------

Translation of ccrB4 ATCC12228    (526) PSTSSLFLPQTLYITIE 542
Translation of ccrB4 HDE288       (443) -----------------
```

C

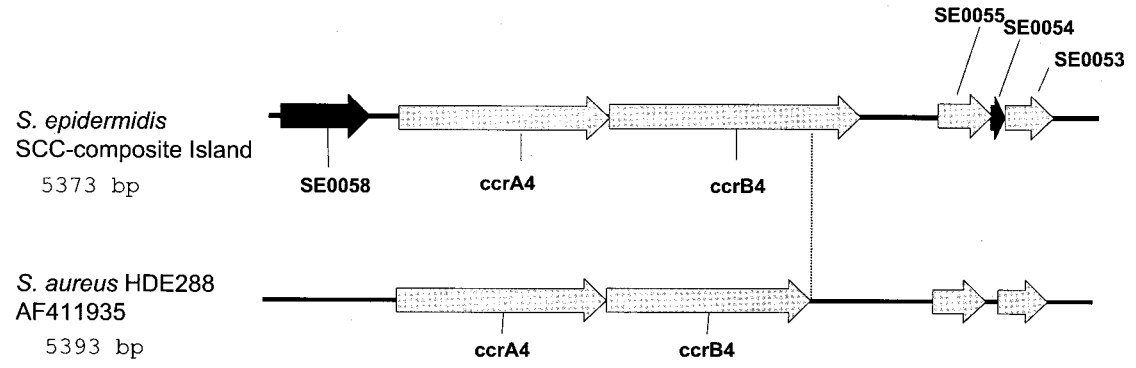

FIG. 6. (A) ClustalW alignment of the *ccrB4* ORF of the SCC composite island of *S. epidermidis* ATCC 12228 (nt 58592 to 60,220 complement) with that of SCC*mec* of strain HDE288 (the pediatric clone) (nt 9184 to 10812, GenBank accession no. AF411935). The missing adenine at position 1326 (shaded dash) of the *ccrB4* ORF of strain HDE288 creates a putative premature stop codon (shaded box). Open box, putative stop codon of the *ccrB4* ORF of strain ATCC 12228. Asterisks indicate identical residues. SCC-CI, SCC composite island. (B) Pairwise comparison of the translated amino acid sequences from the *ccrA4* and *ccrB4* genes of the SCC composite island of *S. epidermidis* ATCC 12228 (see supplemental Table 2 [http://www.ucch.org/daum-boyle_lab-composite_island_figures/table2.htm]) and of strain HDE288 SCC*mec* (accession no. AF411935). These strains showed 91.2% similarity and 87.2% identity for CcrA4 and 80.4% similarity and 80.1% identity for CcrB4. The pairwise alignments were performed by using the Vector NTI suite, version 8 (Informax, Inc.), with the blosum62mt2 matrix. A pairwise ClustalW alignment of the DNA sequences from the entire 5.3-kb region of homology surrounding the *ccrAB4* genes of the SCC composite island of *S. epidermidis* ATCC 12228 (nt 57056 to 62395 complement, accession no. AE016744) and SCC*mec* of strain HDE288 (the pediatric clone) (nt 6986 to 12345, GenBank accession no. AF411935) is shown in supplemental Fig. 6D (available at http://www.ucch.org/daum-boyle_lab-composite_island_figures/fig_6D.htm). (C) Map of the region of nucleotide conservation between the SCC composite island and strain HDE288 that encompasses the *ccrA4* and *ccrB4* genes, highlighting the larger size of the *ccrB4* ORF in the SCC composite island (1,629 versus 1,329 bp, encoding 542 versus 453 aa, respectively; vertical line indicates premature stop codon in strain HDE288). Solid arrows, unique ORFs in the SCC composite island.

ing ORF 13 in *S. hominis* ATCC 27844 and SCC*mec* type I in the MRSA strain NCTC 10442. In summary, there was a tendency for an ORF from the L-C HR to be conserved in a greater number of SCC elements when the position of the ORF in *S. epidermidis* was closer to the *ccr* genes.

(iii) *ccr* gene comparisons. An alignment was performed between the two sets of *ccrAB* genes in CA-MRSA strain 2314 and SCC*pbp4* and genes of *ccrAB* allotypes 1, 2, 3, and 4. The *ccrA* gene identified in isolate 2314 was 98% identical to those of SCC_{pbp4} and CA-MRSA strain CA05 and was 96 to 97% identical to the *ccrA2* alleles of isolates MW2, N315, and 8/6-3P. The *ccrB* gene was also 96 to 97% identical to the *ccrB2* alleles of isolates 8/6-3P, N315, MW2, and CA05, in contrast to 92% homology to that of ATCC 12228. Thus, the *ccrA* and *ccrB* genes in CA-MRSA strain 2314 and SCC*pbp4* are related to the type 2 *ccr* gene allotype, a feature of type IV and type II SCC*mec* elements.

Pairwise comparison of the translated amino acid sequences from the *ccrA4* and *ccrB4* genes of the SCC composite island and SCC*mec* of strain HDE288 (accession no. AF411935) revealed that *ccrA4* had 91.2% similarity and 87.2% identity, and *ccrB4* had 80.4% similarity and 80.1% identity, between these strains (Fig. 6B). In the SCC composite island, the *ccrB4* ORF was larger than that of strain HDE288 (1,629 versus 1,329 bp, encoding 542 versus 453 amino acid [aa] residues, respectively) due to the deletion of a single nucleotide (adenine) at position 1326 of the latter ORF (Fig. 6A).

DISCUSSION

We found a novel 57-kb composite island in *S. epidermidis* strain ATCC 12228 (the SCC composite island) that may represent a primordial genetic element contributing DNA sequences to the SCC*mec* elements found in *S. aureus*. The island has two sets of *ccr* recombinases and a $DR_{SCC\ composite\ island}$ sequence at either end closely resembling the IR_{SCC}-R and DR_{SCC}-R sequences found in SCC*mec* elements in *S. aureus*. Moreover, a smaller (19-kb) SCC element called SCC*pbp4* is nested within the right side of the SCC composite island. The *mecA* gene itself and the genes responsible for its regulation were notably absent.

The SCC composite island had several large regions of substantial homology with SCC*mec* elements (summarized in Fig. 3). A 6.9-kb area in the L-C region of SCC*pbp4* was nearly identical to the L-C region of SCC*mec* type IV elements of CA-MRSA strain 2314 and HA-MRSA strain MR108. This region also shared homology with the SCC element of *S. hominis*. Also, the left side of the island contained a ca. 10-kb stretch of DNA with 92% similarity to a region within SCC*mec* type III (10) that has mercury resistance genes flanked on either end by IS*431*. The CadR region of the SCC composite island contained a 2.5-kb stretch of similarity to the type III element. Also, a highly homologous region of ca 5.3 kb that included the *ccrAB4* genes was present in both the SCC composite island and the SCC*mec* element of MRSA isolate HDE288. Thus, >25 kb of the 57-kb DNA sequence of the SCC composite island was conserved in other SCC*mec* elements. The presence of these regions of virtual identity to two distinct SCC*mec* element types suggests that there has been extensive horizontal genetic exchange between this SCC composite island in *S. epidermidis* and the SCC*mec* elements found in MRSA isolates.

The SCC composite island is unique within this family in several regards. First, within the SCC composite island are two pairs of *ccrA* and *ccrB* genes of different allotypes (types 2 and 4). One pair was within the nested element SCC*pbp4*. Second, several novel arrangements of the DR_{SCC} and IR_{SCC} sequences were present. The 28-bp direct repeat sequence ($DR_{SCC\ composite\ island}$) that flanks the SCC is composed of exact copies of the overlapping composite island $DR_{SCCpbp4}$-R and $IR_{SCCpbp4}$-R sequences, whereas in SCC*mec* elements, the structures of the DR_{SCC} and IR_{SCC} sequence junctions differ slightly at the left and right extremities. Moreover, a third copy of this $DR_{SCC\ composite\ island}$ was present overlapping with the SCC*pbp4* left terminal repeat sequences. This presence of a direct repeat at the margins of the SCC composite island is similar to the architecture of the ends of pathogenicity islands in bacteria (7). The terminal-repeat sequences of the nested SCC*pbp4* element were more typical of SCC*mec* elements. However, the $DR_{SCC\ composite\ island}$ sequence (i.e., an IR/DR_{SCC}-R terminal-repeat sequence) overlapping the $DR/IR_{SCCpbp4}$-L sequence was atypical (Fig. 3). Previously, the left and right terminal repeats had been detected at least 20 kb apart at the left and right termini of SCC elements, respectively. The overlap created a novel 55-bp sequence flanked by a B-bp complementary inverted repeat in the intergenic region between SCC*pbp4* and the left portion of the SCC composite island, downstream of an ORF encoding a phage resistance protein (a probable restriction protein). The significance of this novel juxtaposition of these repeats at the junction of SCC*pbp4* remains to be determined. It is possible that this sequence contains a transcriptional terminator for the phage resistance protein.

The SCC composite island and the nested SCC*pbp4* element are the third and fourth members of the family of SCC elements identified to date that have intact *ccrA* and *ccrB* genes and the characteristic direct- and inverted-repeat sequences. These are features previously shown to allow excision and integration of the element (12). SCC*cap1* (15) is another member of this family, but it lacks a *ccrA* gene homolog, limiting its potential for excision and spread. In this regard, the *ccrAB2* allotype is the only allotype to date shown to mediate excision activity. The functionality of the *ccrAB4* allotype has not yet been investigated, but the *ccrB4* gene in the SCC composite island of ATCC 12228 appears to be more intact than that of HDE288, which has a truncated *ccrB* gene (see Fig. 6).

The presence of cadmium and mercury resistance genes, also present in other SCC*mec* elements, suggests that SCC elements are also used by staphylococci for horizontal transfer of genes encoding resistance to heavy metals. The presence of restriction system genes in the SCC composite island both within and outside SCC*pbp4* suggests that at some time, both portions of the element were transferable between bacterial species.

It remains to be determined whether the SCC composite island is a feature only of *S. epidermidis* ATCC 12228 or whether it can be found among other *S. epidermidis* isolates. If it is common, it is possible that *S. epidermidis*, a skin commensal, acts as a reservoir of DNA sequences that have been horizontally transferred and recombined within SCC*mec* ele-

ments by homologous recombination. It was recently proposed that an SCC element found in *S. hominis* was an ancestral element providing sequences for SCC*mec* elements (13). Our data describe two additional possible ancestral SCC elements present in a commensal staphylococcal species that could also act as a source of DNA for SCC*mec* elements. In this regard, the SCC_{12263} element in *S. hominis* carries type 1 *ccr* genes, whereas the SCC composite island in *S. epidermidis* carries type 2 and 4 *ccr* genes. Thus, *S. epidermidis* and *S. hominis* would be able to provide diversity to SCC*mec* elements by contributing to their different types of *ccr* genes. In this regard, the GC content of SCC elements is very close to that of staphylococcal genomes, supporting the notion that the elements have indeed likely originated from staphylococcal species.

It is not known how SCC elements are horizontally transferred between *S. aureus* strains and other *Staphylococcus* species. The SCC*pbp4* and SCC*mec* elements both carry important cell wall synthesis genes, and SCC*cap1* carries genes responsible for a capsular polysaccharide. These data suggest that SCC elements are specialized elements in staphylococci that carry genes encoding cell wall synthesis enzymes. In this scenario, SCC*mec* elements have been exploited for the transfer of antibiotic resistance by importation of a PBP gene with low affinity for β-lactams. The biological importance of carrying PBP genes such as these on presumably mobile genetic elements remains to be determined but could account for the functional redundancy of PBPs in staphylococci.

Inspection of the aligned maps of tandem ORFs located adjacent to the *ccr* genes in SCC*mec* elements suggests a model in which SCC*mec* elements evolved from the SCC*pbp4* element in *S. epidermidis* (Fig. 2). Isolated in 1996, Dallas CA-MRSA isolate 2314 was one of the first CA-MRSA isolates to be recognized. All five ORFs positioned between the *ccr* genes and the $DR_{SCCpbp4}$-L sequence were present in the L-C region of this isolate and the HA-MRSA strain MR108. The type IV SCC*mec* elements from more-recent CA-MRSA isolates such as MW2, CA05, and 8/6-3P have remnants of ORF 5 but do not contain ORFs 1, 2, 3, and 4. Furthermore, ORFs 3, 4, and 5, upstream of *ccrA* in CA-MRSA isolate 2314, were more closely related to the corresponding ORFs found in HA-MRSA strains bearing SCC*mec* type II. Thus, the ORFs in this region that were closer to the *ccr* genes were more likely to be conserved among a greater range of SCC element types than those more distal to the *ccr* genes. These data also suggest that recombination events have resulted in gradual elimination of ORFs 1, 2, 3, and 4 from SCC*mec* as SCC*mec* type II evolved into SCC*mec* type IVc and ultimately types IVa and IVb.

The left portion of the novel SCC*pbp4* element in SCC*mec* type IVc provides evidence that, at some point, there was horizontal genetic exchange between the progenitors of CA-MRSA strain 2314 and *S. epidermidis* ATCC 12228. It is not clear whether isolate 2314 obtained the L-C portion of SCC*mec* IVc from the SCC*pbp4* element of ATCC 12228 or vice versa. A model whereby homologous pairing occurred between the DR_{SCC} and *ccr* gene sequences of the two SCC elements, resulting in gene replacement in the L-C region of a previously extant SCC*mec* cassette, is one plausible explanation.

ACKNOWLEDGMENTS

S.B. and R.S.D. are the recipients of R01 AI40481-01A1 from NIAID, RO1 CCR523379 from the CDC, and support from the Grant Health Care Foundation. S.B. was also supported by R03 AI44999-01 from NIAID. K.M. was supported by a grant from the Children's Research Foundation, Northbrook, Ill.

REFERENCES

1. **Adcock, P. M., P. Pastor, F. Medley, J. E. Patterson, and T. V. Murphy.** 1998. Methicillin-resistant *Staphylococcus aureus* in two child care centers. J. Infect. Dis. **178:**577–580.
2. **Altschul, S. F., T. L. Madden, A. A. Schaffer, J. Zhang, Z. Zhang, W. Miller, and D. J. Lipman.** 1997. Gapped BLAST and PSI-BLAST: a new generation of protein database search programs. Nucleic Acids Res. **25:**3389–3402.
3. **Baba, T., F. Takeuchi, M. Kuroda, H. Yuzawa, K. Aoki, A. Oguchi, Y. Nagai, N. Iwama, K. Asano, T. Naimi, H. Kuroda, L. Cui, K. Yamamoto, and K. Hiramatsu.** 2002. Genome and virulence determinants of high virulence community-acquired MRSA. Lancet **359:**1819–1827.
4. **Daum, R. S., T. Ito, K. Hiramatsu, F. Hussain, K. Mongkolrattanothai, M. Jamklang, and S. Boyle-Vavra.** 2002. A novel methicillin-resistance cassette in community-acquired methicillin-resistant *Staphylococcus aureus* isolates of diverse genetic backgrounds. J. Infect. Dis. **186:**1344–1347.
5. **Domanski, T. L., and K. W. Bayles.** 1995. Analysis of *Staphylococcus aureus* genes encoding penicillin-binding protein 4 and an ABC-type transporter. Gene **167:**111–113.
6. **Fey, P. D., B. Said-Salim, M. E. Rupp, S. H. Hinrichs, D. J. Boxrud, C. C. Davis, B. N. Kreiswirth, and P. M. Schlievert.** 2003. Comparative molecular analysis of community- or hospital-acquired methicillin-resistant *Staphylococcus aureus.* Antimicrob. Agents Chemother. **47:**196–203.
7. **Hacker, J., and J. B. Kaper.** 2000. Pathogenicity islands and the evolution of microbes. Annu. Rev. Microbiol. **54:**641–679.
8. **Henze, U. U., and B. Berger-Bachi.** 1995. *Staphylococcus aureus* penicillin-binding protein 4 and intrinsic β-lactam resistance. Antimicrob. Agents Chemother. **39:**2415–2422.
9. **Hiramatsu, K., K. Okuma, X. X. Ma, K. Yamamoto, S. Hori, and M. Kapi.** 2002. New trends in *Staphylococcus aureus* infections: glycopeptide resistance in hospital and methicillin resistance in the community. Curr. Opin. Infect. Dis. **15:**407–413.
10. **Ito, T., Y. Katayama, K. Asada, N. Mori, K. Tsutsumimoto, C. Tiensasitorn, and K. Hiramatsu.** 2001. Structural comparison of three types of staphylococcal cassette chromosome *mec* in the chromosome of methicillin-resistant *Staphylococcus aureus.* Antimicrob. Agents Chemother. **45:**1323–1336.
11. **Ito, T., K. Okuma, X. X. Ma, H. Yuzawa, and K. Hiramatsu.** 2003. Insights on antibiotic resistance of *Staphylococcus aureus* from its whole genome: genomic island SCC. Drug Resist. Updat. **6:**41–52.
12. **Katayama, Y., T. Ito, and K. Hiramatsu.** 2000. A new class of genetic element, staphylococcus casette chromosome *mec*, encodes methicillin resistance. Antimicrob. Agents Chemother. **44:**1549–1555.
13. **Katayama, Y., F. Takeuchi, T. Ito, X. X. Ma, Y. Ui-Mizutani, I. Kobayashi, and K. Hiramatsu.** 2003. Identification in methicillin-susceptible *Staphylococcus hominis* of an active primordial mobile genetic element for the staphylococcal cassette chromosome *mec* of methicillin-resistant *Staphylococcus aureus.* J. Bacteriol. **185:**2711–2722.
14. **Kuroda, M., T. Ohta, I. Uchiyama, T. Baba, H. Yuzawa, I. Kobayashi, L. Cui, A. Oguchi, K.-I. Aoki, Y. Nagai, J.-Q. Lian, T. Ito, M. Kanamori, H. Matsumaru, A. Maruyama, H. Murakami, A. Hosoyama, Y. Mizutani-Ui, N. K. Takahashi, T. Sawano, R.-I. Inoue, C. Kaito, K. Sekimizu, H. Hirakawa, S. Kuhara, S. Goto, J. Yabuzaki, M. Kanehisa, A. Yamashita, K. Oshima, K. Furuya, C. Yoshino, T. Shiba, M. Hattori, N. Ogasawara, H. Hayashi, and K. Hiramatsu.** 2001. Whole genomic sequencing of methicillin-resistant *Staphylococcus aureus*. Lancet **357:**1225–1240.
15. **Luong, T. T., S. Ouyang, K. Bush, and C. Y. Lee.** 2002. Type 1 capsule genes of *Staphylococcus aureus* are carried in a staphylococcal cassette chromosome genetic element. J. Bacteriol. **184:**3623–3629.
16. **Ma, X. X., T. Ito, C. Tiensasitorn, M. Jamklang, P. Chongtrakool, S. Boyle-Vavra, R. S. Daum, and K. Hiramatsu.** 2002. A novel type of staphylococcal cassette chromosome *mec* (SCC*mec*) identified in community-acquired methicillin-resistant *Staphylococcus aureus* strains. Antimicrob. Agents Chemother. **46:**1147–1152.

16a. **Mongkolrattanothai, K., S. Boyle, M. D. Kahana, and R. S. Daum.** 2003. Severe *Staphylococcus aureus* infections caused by clonally related community-acquired methicillin-susceptible and methicillin-resistant isolates. Clin. Infect. Dis. **37:**1050–1058.

17. **Niemeyer, D. M., M. J. Pucci, J. A. Thanassi, V. K. Sharma, and G. L. Archer.** 1996. Role of *mecA* transcriptional regulation in the phenotypic expression of methicillin resistance in *Staphylococcus aureus.* J. Bacteriol. **178:**5464–5471.
18. **Okuma, K., K. Iwakawa, J. D. Turnidge, W. B. Grubb, J. M. Bell, F. G. O'Brien, G. W. Coombs, J. W. Pearman, F. C. Tenover, M. Kapi, C. Tien-**

sasitorn, T. Ito, and K. Hiramatsu. 2002. Dissemination of new methicillin-resistant *S. aureus* clones in the community. J. Clin. Microbiol. **40:**4289–4294.
19. **Oliveira, D. C., and H. de Lencastre.** 2002. Multiple PCR strategy for rapid identification of structural types and variants of the *mec* element in methicillin-resistant *Staphylococcus aureus.* Antimicrob. Agents Chemother. **46:**2155–2161.
20. **Oliveira, D. C., A. Tomasz, and H. de Lencastre.** 2001. The evolution of pandemic clones of methicillin-resistant *Staphylococcus aureus*: identification of two ancestral genetic backgrounds and the associated *mec* elements. Microb. Drug Resist. **7:**349–361.
21. **Thompson, J. D., D. G. Higgins, and T. J. Gibson.** 1994. CLUSTAL W: improving the sensitivity of progressive multiple sequence alignment through sequence weighting, position-specific gap penalties and weight matrix choice. Nucleic Acids Res. **22:**4673–4680.
22. **Wisplinghoff, H., A. E. Rosato, M. C. Enright, M. Noto, W. Craig, and G. L. Archer.** 2003. Related clones containing SCC*mec* type IV predominate among clinically significant *Staphylococcus epidermidis* isolates. Antimicrob. Agents Chemother. **47:**3574–3579.
23. **Zhang, H. Z., C. J. Hackbarth, K. M. Chansky, and H. F. Chambers.** 2001. A proteolytic transmembrane signaling pathway and resistance to beta-lactams in staphylococci. Science **291:**1962–1965.
24. **Zhang, Y. Q., S. X. Ren, H. L. Li, Y. X. Wang, G. Fu, J. Yang, Z. Q. Qin, Y. G. Miao, W. Y. Wang, R. S. Chen, Y. Shen, Z. Chen, Z. H. Yuan, G. P. Zhao, D. Qu, A. Danchin, and Y. M. Wen.** 2003. Genome-based analysis of virulence genes in a non-biofilm-forming *Staphylococcus epidermidis* strain (ATCC 12228). Mol. Microbiol. **49:**1577–1593.